Received February 16, 2022, accepted March 20, 2022, date of publication March 25, 2022, date of current version April 4, 2022.

Digital Object Identifier 10.1109/ACCESS.2022.3162269

Explicit Model Predictive Based Fault Tolerant Control for Turboshaft Engine System

NANNAN GU[1], XI WANG[1,2], AND SHUBO YANG[1]
[1]School of Energy and Power Engineering, Beihang University, Beijing 100191, China
[2]Collaborative Innovation Center for Advanced Aero-Engine, Beijing 100191, China

Corresponding author: Shubo Yang (xjysb@qq.com)

This work was supported by the National Science and Technology Major Project under Grant 2017-V-0015-0067.

ABSTRACT In order to tackle the faults of turboshaft engine-rotor systems and the real time implementation difficulty of traditional model predictive control methods, an explicit model predictive (EMPC) fault-tolerant control algorithm is designed based on an active fault-tolerant control scheme that implicitly detects the faults and adjusts the control law online. The proposed real time control algorithm can achieve good control command tracking performance and, at the same time, guarantee limit protection of turboshaft engine-rotor system. Firstly, to start with the algorithm, a dynamic system model library and a fault monitoring mechanism are established, in which the dynamic system model library contains sets of piecewise affine models (PWA) of normal engine mode and modes with faults. Secondly, the EMPC fault-tolerant controller is derived and designed for each sub-model in the modes of dynamic model library. Through the transformation and derivation of the traditional model predictive controller of turboshaft engine-rotor system, the explicit solution of its fault-tolerant controller is obtained. With the explicit solution which is in the form of state feedback control for each partition, controller gains can be designed off-line. Finally, the online engine control process is completed by searching the corresponding controller gain based on engine state, which improves the real-time performance of the control system. The effectiveness of the method for engine systems with modeled or un-modeled compressor faults and the robustness of the algorithm are verified by simulations.

INDEX TERMS Explicit model predictive control, fault tolerant control, turboshaft engine-rotor system, limit protection.

I. INTRODUCTION

Turboshaft engines are the main power units of most active helicopters in the world. And they always work under very harsh conditions such as extremely high temperature, pressure and large stress [1]. At the same time, compared with other types of aeroengines, turboshaft engines also need to work with large rotor loads that may vary from time to time. These working requirements introduce great difficulties to the design of turboshaft engine controllers which has to constrain system states within safe region. In addition to which, engines may suffer from performance degradation resulting from engine faults like components damage or foreign object damage. This could bring uncertainties to the system controller. Therefore, the design of turboshaft engine control system must not only meet the design requirements of steady-state and transition state control under harsh working conditions, but also have high reliability and fault tolerance ability [2]. And MPC control could be a good choice.

TABLE 1. Parameter symbol table.

Symbol	Name
n_g	Gas turbine speed
n_{g0}	Gas turbine speed at equilibrium point
n_p	Power turbine speed
n_{p0}	Power turbine speed at equilibrium point
T_4	Gas turbine inlet temperature
T_{40}	Gas turbine inlet temperature at equilibrium point
$xcpc$	Collective pitch input of rotor system
$xcpc_0$	Collective pitch input at equilibrium point
w_f	Engine fuel input
w_{f0}	Engine fuel input at equilibrium point
H	Helicopter flight altitude
Ma	Helicopter flight Mach number
N_y	Prediction horizon
N_u	Control horizon

The associate editor coordinating the review of this manuscript and approving it for publication was Jingang Jiang.

The idea of MPC control originated in the 1970s. It is a kind of control algorithm to meet the needs of industry for the control of multi-input systems with constrained conditions problems. And then due to its unique advantages such as the ability to predict future output, process constrained optimization, and suppress unmodeled dynamic error and environmental disturbance uncertainty, it has been widely applied in industry. In April 2019, a report issued by the International Control Union further verified the importance of the MPC algorithm, which pointed out that after five years time, MPC is expected to overtake PID to be the most widely used control algorithm in industry [3]. At present, there are many papers on the application of MPC in process control and the improvement of related academic theories and algorithms. [4]–[6] describe in detail the application process of MPC in industrial process control such as petroleum smelting and chemical industry. Meanwhile, MPC has also been used in large machineries, such as wind power generator [7] and heavy duty diesel engine [8]. [9], [10] give a detailed derivation process on the improvement and robustness of the MPC algorithm from a theoretical point of view. In recent years, the application research of MPC in Aeroengine has also made a great breakthrough.

But unlike other systems(wind power generator, heavy duty diesel engine and process control system), turboshaft engine-rotor system is a kind of relatively special system. This system is more complex building from more components including inlet, compressor, combustor, turbine, nozzle etc. The engine and rotor components are highly coupled. The dynamics of which is fast with large lag factor involved, which suggest new challenges to application of MPC algorithm on it. Maciejowsji and Jones [11] argued that MPC can not only be used for managing engine constraints, but can also solve the problem caused by large dynamic lag. The large dynamic lag resulting from large inertial rotor link has always been the biggest problem to be solved in the design of turboshaft engine-rotor system control system. Saluru and Yedavalli proposed the idea of replacing traditional PID with MPC and verified its effectiveness in [12], which showed that the technology can be implemented on aeroengines. Although there have been such progress as discussed above, there still remain two problems to be solved urgently regarding the application of the MPC algorithm on aero-engines: the real-time implementation and the fault tolerance of the algorithm.

In order to solve the real time application problem introduced by large amount of online calculation of MPC, Bemporad proposed the EMPC algorithm based on multi-parameter quadratic programming theory in [13]. Parametric programming is a kind of optimization problem with parameters, in which multi-parameter quadratic programming is popular in academia because of its convexity [14], [15]. By the partition of the parameter space, the multi-parameter quadratic programming has the ability to obtain the explicit controller off-line, which can simplify the process of on-line control [16]–[18]. The EMPC based on parametric quadratic programming can reduce the online computing time to meet the real-time requirements. However, considering the particularity of turboshaft engine-rotor system, MPC application on such system is relative rare and the EMPC results are even fewer.

Considering the high real-time requirements of turboshaft engine rotor system control system, this paper will design a turboshaft engine controller based on EMPC to solve the problem which is that traditional MPC can not guarantee real-time performance. On top of which, we will also take engine faults into consideration and design a real time fault tolerant control algorithm. The algorithm will be described in the following paragraph.

Based on the component-level nonlinear simulation model of turboshaft engine-rotor system, this paper first constructs a dynamic model library and a fault monitoring mechanism. The dynamic model library includes PWA models under both normal and fault engine modes. And through theoretical derivation, an EMPC controller is designed for each sub-model of the PWA models in the dynamic model library. The individual controller design process of turboshaft engine proposed in this paper is that: Firstly, parameter space consisting of system states is reasonably partitioned. After which by derivation introduced in this paper, the detailed piecewise affine linear function relationship between the controller and the related parameters on each parameter partition is obtained, which is later proved to be in the form of state feedback control for each partition. These are all done in offline step. With those designed controllers, during online implementation process, the optimal control decision of turboshaft engine-rotor system is obtained by selecting corresponding sub-system EMPC controller and querying the partition of system state. As described above, the online control procedure will only require small amount of resource for querying and linear calculation. The real time performance can be guaranteed. The later simulation results show the effectiveness and robustness of the proposed controller for turboshaft engines with known or unknown compressor faults.

Contributions: The contributions of this paper are: (1) This paper has suggested an EMPC algorithm for the control of turboshaft engine with taking engine faults into consideration. The theory analysis and design process are carefully discussed and illustrated through derivation. (2) Different from traditional controllers for aircraft engines (PID controller with MIN-MAX selection logic), the EMPC based algorithm presented in this paper can design a simpler and more straightforward controller without complex selection logic required by traditional control algorithms; (3) Compared with conventional MPC, the proposed EMPC algorithm improve real-time capability which is of significant importance for aero engine.

The rest of the paper is organized as follows: Section II briefly introduces the turboshaft engine-rotor system and its control problem description. Section III presents the EMPC fault tolerant algorithm for the turboshaft

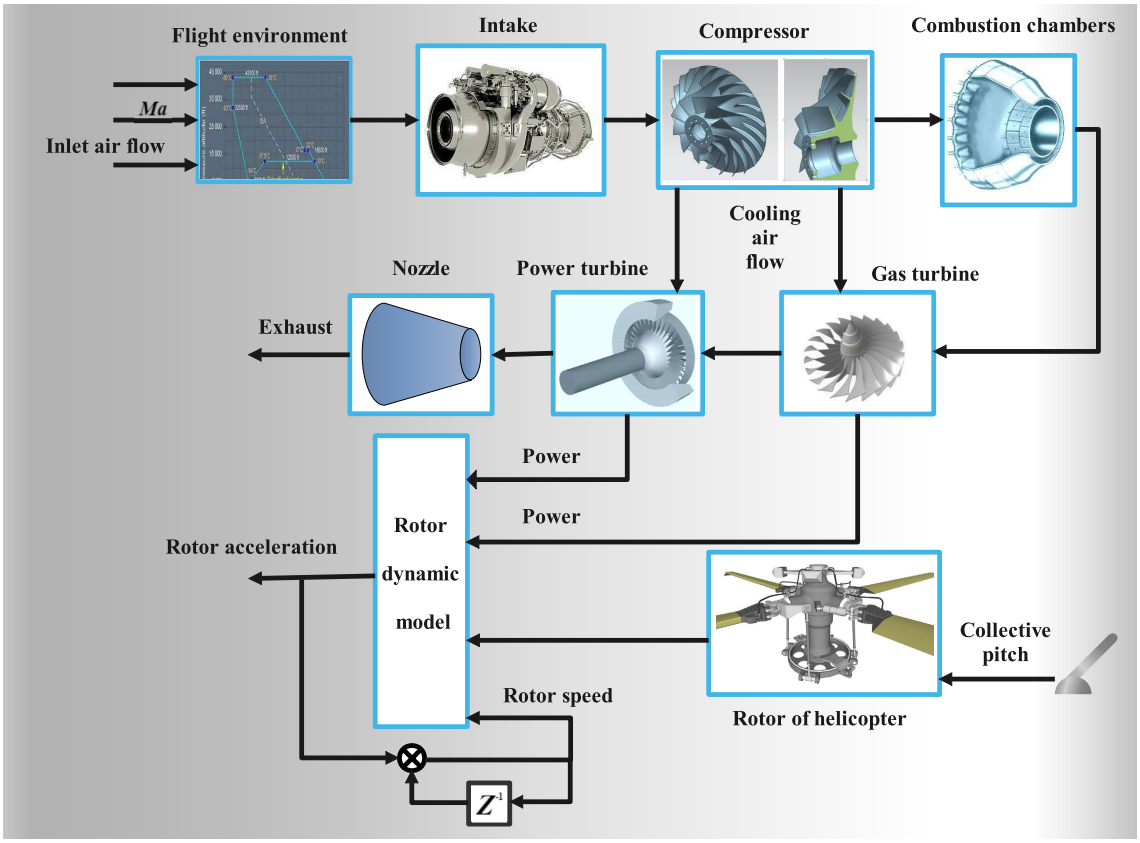

FIGURE 1. The structure diagram of turboshaft engine-rotor system.

engine-rotor system. In Section IV, a simulation study on a turboshaft engine-rotor system is presented to verify the proposed method. Finally, Section V concludes the paper.

II. TURBOSHAFT ENGINE-ROTOR SYSTEM AND PROBLEM DESCRIPTION

We will introduce the to-be controlled turboshaft engine system and the control problem description in this section.

A. TURBOSHAFT ENGINE-ROTOR SYSTEM

The dynamic process of turboshaft engine-rotor system is highly nonlinear and has strong engine-rotor coupling characteristics. Its model is usually a component-level nonlinear one based on thermal-dynamics, aerodynamics and iterative solution method (Fig.1). There is no explicit linear expression between system inputs and outputs. The following state space nonlinear equations are often used to describe the turboshaft engine-rotor dynamics between system inputs and state parameters:

$$\begin{bmatrix} \dot{n_g} \\ \dot{n_p} \end{bmatrix} = f\left(\begin{bmatrix} n_g \\ n_p \end{bmatrix}, w_f, xcpc, H, Ma\right) \tag{1}$$

where $\begin{bmatrix} n_g \\ n_p \end{bmatrix}$ is the state vector of the system. n_g and n_p are gas turbine speed and power turbine speed respectively. The control input is the turboshaft engine fuel flow w_f. The collective pitch of rotor system $xcpc$, the flying altitude H, and the flight Mach number Ma are considered as disturbance inputs in this paper. Based on the state and input parameters relationship of turboshaft engine-rotor system shown in Fig.1 and equation (1), in order to complete the fault-tolerant controller design, PWA modeling method is considered to obtain the explicit linear relationship between system inputs and states. Firstly, the nonlinear model of turboshaft engine-rotor system is linearized at the ground state. At s steady-state operating point, the discrete PWA model of turboshaft engine-rotor system is established as follows:

$$\begin{cases} \Delta n^i(k+1) = A^i \Delta n^i(k) + B^i \Delta {w_f}^i(k) \\ \quad + B_w^i \Delta xcpc^i(k) \\ \Delta y^i(k) = C^i \Delta n^i(k)^i + D^i \Delta {w_f}^i(k) \\ \quad + D_w^i \Delta xcpc^i(k) \end{cases} \tag{2}$$

where, $\Delta n^i(k) = \begin{bmatrix} n_g(k) \\ n_p(k) \end{bmatrix}^i - \begin{bmatrix} n_{g0} \\ n_{p0} \end{bmatrix}^i$, $\Delta {w_f}^i(k) = {w_f}^i(k) - {w_{f0}}^i$, $\Delta xcpc^i(k) = xcpc^i(k) - xcpc^i{}_o$. n_{g0}^i, n_{p0}^i, w_{f0}^i, $xcpc_0^i$ are the equilibrium points corresponding to the parameters on the i-th linear system and explained in Table 1 in detail.

Note1: High altitude and other flight conditions can be transformed into ground states by similarity theory, so as to realize the full flight envelope control of engine.

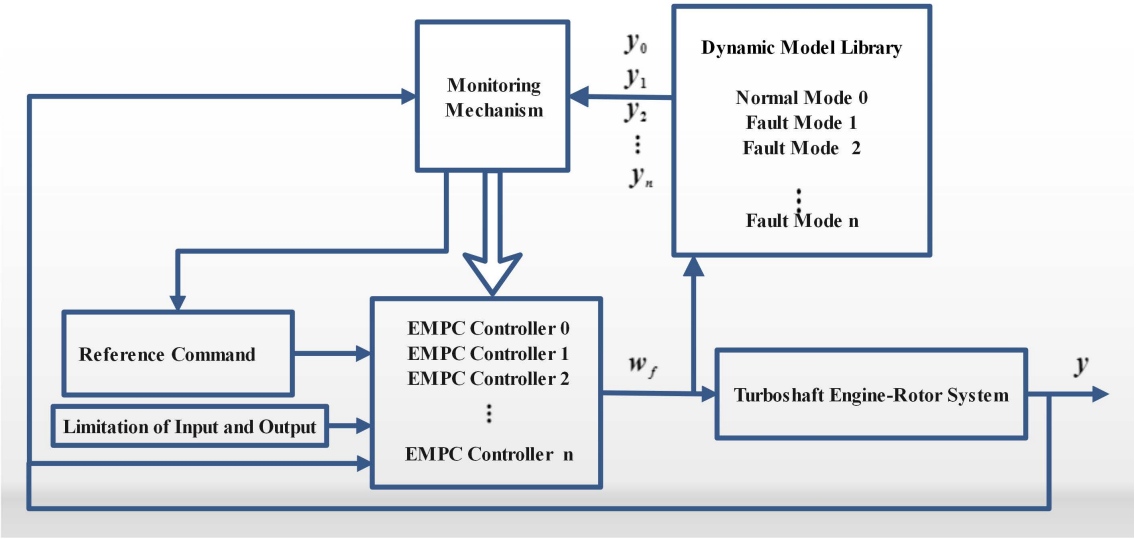

FIGURE 2. The procedure schematic diagram of EMPC active fault tolerant controller.

Note2: The modeling method of PWA model of turboshaft engine-rotor system is as follows: Firstly, the equilibrium point is extracted; then the linear system near the equilibrium point is modeled based on the small deviation method; and finally the scheduling modeling of PWA system is completed based on the variable geometry scheduling strategy.

B. PROBLEM DESCRIPTION

1) FAULTS TYPE

The faults resulting in the performance degradation of engine components can be modeled as the decline of efficiency and mass flow factor(flow capacity) of each component. In this paper, compressor fault is taken as an example for known faults with a prior knowledge modeled by the change of compressor mass flow factor. In order to highlight the necessity of fault-tolerant control, large compressor faults are selected for explanation: the mass flow factor decreases by 3%, 5% and 7% respectively [19]. Other types of faults can be managed in the same way and will not discussed in this paper.

2) LIMITATION PROTECTION

The engine control system should not only realize the steady-state control function, but also meet the requirements of restricted parameters protection in the process of transition state flight, so as to ensure that the engine always works within the safe range. During the transition state of turboshaft engine-rotor system, the main protection requirements to be considered are as follows:

1) The maximum and minimum fuel flow limits of engine:

$$w_{f,\min} \leq w_f \leq w_{f,max} \tag{3}$$

2) In order to avoid the burst of turbine disk, damage to the turbine blades, or high temperature shortening the life of components, gas turbine inlet temperature limit and the gas turbine speed limit need to be considered:

$$\begin{aligned} T_4 &\leq T_{4,max} \\ n_g &\leq n_{g,max} \end{aligned} \tag{4}$$

Among them, the meaning of the parameters can be referred to Table 1. And the subscripts *max* and *min* represent the maximum and minimum values of the corresponding parameters respectively.

3) THE OBJECT OF FAULT TOLERANT CONTROL

The purpose of fault-tolerant control in this paper is to ensure that the power turbine speed is constant under different flight missions by adjusting the fuel flow in case of compressor faults (compressor mass flow factor degradation [19]), so as to meet the demand of helicopter rotor system for propellers power load change. At the same time, it needs to be ensured that the acceleration and deceleration time during the transition state is as short as possible, and the key parameters described above i.e. fuel flow, gas turbine inlet temperature and turboshaft speed do not exceed the limit.

III. EMPC ACTIVE FAULT TOLERANT CONTROL

The design of EMPC fault-tolerant controller mainly includes three aspects: the establishment of dynamic model library, the monitoring mechanism and the design of EMPC controller. The control procedure schematic diagram is shown in Fig. 2. The dynamic library provides data for monitoring mechanism module which will decide current engine mode. Based on engine mode given by monitoring module, the controller module will output control command by selecting specific off-line designed EMPC controller. We will now describe these modules in detail in the following sections.

A. ESTABLISHMENT OF DYNAMIC MODEL LIBRARY

The dynamic model library is used to store the PWA models and predict next time step engine states under engine normal and fault modes. This module's outputs provide inputs for the monitoring mechanism unit to assist it in judging the state of the engine at the moment. As stated before this article takes compressor fault as an example. Other faults types are the same. As a known fault with prior knowledge, compressor fault is generally simulated by the change of mass flow factor or efficiency factor. In order to highlight the necessity and importance of fault tolerance, this paper selects three different degradation scales (3%, 5%, 7%) of compressor mass flow factor for fault modeling and simulation, and establishes the corresponding PWA model for the engine under different degradation rates. Hence the dynamic library contains four PWA models for compressor normal mode and three fault modes.

B. DESIGN OF MONITORING MECHANISM

The real nonlinear engine output and the output of each PWA in the dynamic model library are monitored in real time. And the quadratic performance index of their error is taken as the detection criterion. The main function of the monitoring mechanism is to decide the mode that can simulate current engine dynamic best. Assuming that the output of the i-th PWA in the dynamic model library at time k is $\widehat{y_i}(k)$ and the output of the engine is $y(k)$, the quadratic error measurement index is defined as follows:

$$\widehat{J_i}(k) = (y(k) - \widehat{y_i}(k))^2, i = 1, 2 \cdots, n \tag{5}$$

The decision indicator can be get as follows:

$$\aleph = \min\left(\widehat{J_i}(k)\right) \tag{6}$$

The flow chart of monitoring mechanism is shown in Figure 3.

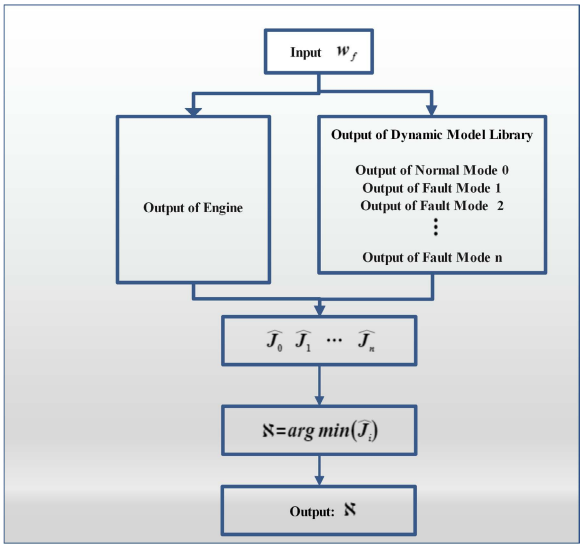

FIGURE 3. The flow chart of monitoring mechanism.

C. DESIGN OF EMPC CONTROLLER

For each sub-model in PWAs from the dynamic model library, we will design an EMPC controller offline. Taking the objective function as the weighted sum of engine tracking error and fuel flow:

$$J = \sum_{j=1}^{N_y} \left\{ \begin{array}{l} [\Delta y(k+j|k) - r(k)]^T Q \left[\Delta y^i(k+j|k) - r(k)\right] \\ +\Delta {w_f}^i(k+j|k)^T R \Delta {w_f}^i(k+j|k) \end{array} \right\} \tag{7}$$

where, r is the controller tracking command. Q and R represent the weighting matrix of tracking error and fuel flow $\Delta {w_f}^i$ respectively. And, $Q \geq 0$, $R > 0$. With those definations, the MPC problem can be described as follows:

$$\begin{aligned} &\min_{\Delta {w_f}^i(k+j|k)} \quad J \\ &s.t.\ \Delta y_{\min} \leq \Delta y(k+j|k) \leq \Delta y_{\max}, \\ &\quad \Delta w_{f\,\min} \leq \Delta w_f((k+j|k)) \leq \Delta w_{f\,\max} \end{aligned} \tag{8}$$

It can be seen from the objective function that increasing N_y (or increasing the eigenvalue of matrix Q) is beneficial to increasing the stability of the system, but the dynamic response speed of the system becomes slower. On the hand, reducing N_y (or reducing the eigenvalue of matrix Q) is conducive to increase the dynamic response speed of the system, but it will reduce the stability of the system at the same time; Increasing the eigenvalue of R will produce a slow dynamic response. If decreasing R eigenvalue, the control quantity can be greatly deteriorated and the system response speed can be accelerated.

The EMPC algorithm is a kind of control algorithm that transforms the model predictive control problem in equation (8) into the standard multi-parameter quadratic programming (mpQP) problem in equation (9) and obtains its explicit solution. Suppose the standard EMPC mathematical expression with parameter Z_1 is:

$$\begin{aligned} &\min_Z \frac{1}{2} Z^T H Z \\ &s.t.\ GZ \leq W + SZ_1 \end{aligned} \tag{9}$$

Theorem 1: Let $Z_1 = \begin{bmatrix} \Delta n^i(k) \\ \overline{\Delta xcpc}^i(k) \\ \overline{r}(k) \end{bmatrix}$, $Z = \overline{\Delta w_f}^i + (\Pi_3)^{-1} * \Pi_2 Z_1$, then, the MPC problem can be converted to the standard multi-parameter quadratic programming form of equation (9), where

$$\begin{aligned} H &= 2\Pi_3 \\ \Pi_2 &= \begin{bmatrix} P^i_{yx} & P^i_{yw} & -I^i \end{bmatrix}^T Q^i P^i_{yu} U^i \\ \Pi_3 &= \left(P^i_{yu}\right)^T Q^i P^i_{yu} + R^i \\ G &= \begin{bmatrix} I & -I\ P^i_{yu} & -P^i_{yu} \end{bmatrix} \end{aligned}$$

$$W = \begin{bmatrix} \begin{bmatrix} I \\ \vdots \\ I \end{bmatrix} \Delta w_{f\max} - \begin{bmatrix} I \\ \vdots \\ I \end{bmatrix} \Delta w_{f\min} \\ \begin{bmatrix} I \\ \vdots \\ I \end{bmatrix} y_{\max} - \begin{bmatrix} I \\ \vdots \\ I \end{bmatrix} y_{\min} \end{bmatrix}$$

$$E = \begin{bmatrix} 0 & 0 & \begin{bmatrix} -P_{yx}^i & -P_{yw}^i & 0 \end{bmatrix} \\ & & \begin{bmatrix} P_{yx}^i & P_{yw}^i & 0 \end{bmatrix} \end{bmatrix}$$

$$S = E + G * (2\Pi_3)^{-1}(2\Pi_2)^T$$

$$\overline{\Delta xcpc}^i(k) = \begin{bmatrix} \Delta xcpc^i(k) \\ \vdots \\ \Delta xcpc^i(k+N_y-1) \end{bmatrix}$$

$$\overline{\Delta w_f}^i(k) = \begin{bmatrix} \Delta {w_f}^i(k) \\ \vdots \\ \Delta {w_f}^i(k+N_y-1) \end{bmatrix}$$

$$\bar{r}(k) = \begin{bmatrix} r(k) \\ \vdots \\ r(k+N_y-1) \end{bmatrix}$$

Proof 1: Firstly, based on the PWA system shown in equation (2), the state prediction equations of the system are calculated as follows:

$$\begin{bmatrix} \Delta n^i(k+1) \\ \vdots \\ \Delta n^i(k+N_y) \end{bmatrix} = P_x^i \Delta n^i(k) + P_u^i \overline{\Delta w_f}^i(k) + P_w^i \overline{\Delta xcpc}^i(k) \tag{10}$$

$$\begin{bmatrix} \Delta y^i(k+1) \\ \vdots \\ \Delta y^i(k+N_y) \end{bmatrix} = \begin{bmatrix} C^i \Delta n^i(k+1) \\ \vdots \\ C^i \Delta n^i(k+N_y) \end{bmatrix} + \begin{bmatrix} D^i \Delta {w_f}^i(k+1) \\ \vdots \\ D^i \Delta {w_f}^i(k+N_y) \end{bmatrix} + \begin{bmatrix} D_w{}^i \Delta xcpc^i(k+1) \\ \vdots \\ D_w{}^i \Delta xcpc^i(k+N_y) \end{bmatrix} = P_{yx}^i \Delta n^i(k) + P_{yu}^i \overline{\Delta w_f}^i(k) + P_{yw}^i \overline{\Delta xcpc}^i(k) \tag{11}$$

Then the output prediction equation of the turboshaft engine-rotor system can be obtained:

See Appendix B for the specific expressions of P_x^i, P_u^i, P_w^i, P_{yx}^i, P_{yw}^i and P_{yu}^i.

Incorporating equations (10)-(11) and Z_1 into the objective function in equation (8), we get:

$$J = \left\{ \begin{bmatrix} P_{yx}^i & P_{yw}^i & -I^i \end{bmatrix} Z_1 + P_{yu}^i \overline{\Delta w_f}^i \right\}^T Q \left\{ \begin{bmatrix} P_{yx}^i & P_{yw}^i & -I^i \end{bmatrix} Z_1 + P_{yu}^i \overline{\Delta w_f}^i \right\} + \overline{\Delta w_f}^{i\,T} R^i \overline{\Delta w_f}^i \tag{12}$$

Let

$$\Pi_1 = \begin{bmatrix} P_{yx}^i & P_{yw}^i & -I^i \end{bmatrix}^T Q^i \begin{bmatrix} P_{yx}^i & P_{yw}^i & -I^i \end{bmatrix}$$

$$\Pi_2 = \begin{bmatrix} P_{yx}^i & P_{yw}^i & -I^i \end{bmatrix}^T Q^i P_{yu}^i U^i$$

$$\Pi_3 = \left(P_{yu}^i\right)^T Q^i P_{yu}^i + R^i$$

then,

$$\min_{\Delta {w_f}^i(k+j|k)} J = {Z_1}^T \Pi_1 Z_1 + \min_{\overline{\Delta w_f}^i(k+j|k)} \left\{ 2{Z_1}^T \Pi_2 \overline{\Delta w_f}^i + \frac{1}{2} \overline{\Delta w_f}^{i\,T} 2\Pi_3 \overline{\Delta w_f}^i \right\} \tag{13}$$

Let $Z = \overline{\Delta w_f}^i + (\Pi_3)^{-1} * \Pi_2 Z_1$, then

$$\min_{\Delta {w_f}^i(k+j|k)} J = \min_Z \frac{1}{2} Z^T H Z \tag{14}$$

where, $H = 2\Pi_3$.

Similarly, the equivalent linear transformation of the restriction problem in equation (8) can be obtained:

$$G\overline{\Delta w_f}^i \le W + E \begin{bmatrix} \Delta n^i(k) \\ \overline{\Delta xcpc}^i(k) \\ \bar{r}(k) \end{bmatrix} \tag{15}$$

Bring $Z = \overline{\Delta w_f}^i + (\Pi_3)^{-1} * \Pi_2 Z_1$ and $S = E + G * (2\Pi_3)^{-1}(2\Pi_2)^T$ into equation (15):

$$GZ \le W + SZ_1 \tag{16}$$

Thus the Theorem 1 is proved.

Note3: Since the MPC control problem in (7)(8) is not a standard mpQP problem, and due to the particularity of turboshaft engine-rotor system, the influence of disturbance input (rotor system input) on the derivation process has to be considered in the conversion of problem (7)(8) to problem (9). Therefore, we need to first convert the MPC problem of turboshaft engine-rotor system into a standard mpQP problem, which is the main role of Theorem 1.

Lemma 1 [18]: For the optimization problem equation (9), the optimal solution $Z(x)$ on any partition of the parameter Z_1 space is continuous and piecewise affine, namely:

$$Z(x) = F_l Z_1 + G_l \tag{17}$$

where, F_l and G_l are the gain matrices of optimal solution that need to be solved.

Lemma 2 [18]: For any partition in the parameter space Z_1, assuming that the optimization problem equation (9) on this partition satisfies both the linear independent restriction condition LICQ and the strict complementary relaxation condition, and there exists an initial feasible

solution $Z_{10} = \begin{bmatrix} \Delta n_0{}^i(k) \\ \overline{\Delta xcpc_0}{}^i(k) \\ \overline{r}_0(k) \end{bmatrix}$ in this partition at the same time, then the feasible solution of the optimization problem on this partition can be expressed as follows:

$$\begin{bmatrix} Z(Z_1) \\ \lambda(Z_1) \end{bmatrix} = -(M_0)^{-1} N_0 (Z_1 - Z_{10}) + \begin{bmatrix} Z_0 \\ \lambda_0 \end{bmatrix} \tag{18}$$

where $M_0 = \begin{bmatrix} 2\Pi_3 & G_1^T & \cdots & G_1^T \\ -\lambda_1 G_1 & -V_1 & \cdots & -V_q \\ \vdots & \vdots & \ddots & \vdots \\ -\lambda_p G_q & -V_1 & \cdots & -V_q \end{bmatrix}$, $N_0 = \begin{bmatrix} Y & \lambda_1 S_1 & \cdots & \lambda_p S_p \end{bmatrix}$, $V_i = G_i Z_0 - W_i - S_i Z_{10}$, G_i, S_i and W_i represent the ith row of matrix G, S, and W respectively. Y is a zero matrix of dimension $s \times n$, $\lambda_0 = \lambda(x_0)$ is a set of nonnegative Lagrange multipliers, $Z_0 = Z(Z_{10})$ is a set of initial feasible solutions of optimization problem (9).

Theorem 2: Let F_l' be the first m rows of matrix $-(M_0)^{-1}N_0$, G_l' be the first m rows of matrix $(M_0)^{-1}N_0 Z_{10} + Z_0$, and m is the number of rows of Z, then the EMPC controller of the turboshaft engine-rotor system is continuous, and its explicit expression on any partition is as follows:

$$\overline{\Delta w_f}^i = F_l Z_1 + G_l,\ F_l = F_l' - (\Pi_3)^{-1} * \Pi_2,\ G_l = G_l' \tag{19}$$

Proof 2: From Lemma 1, we can see that the EMPC controller of turboshaft engine-rotor system is continuous. Based on Lemma 2, $Z(Z_1) = F_l' Z_1 + G_l'$. And because $Z = \overline{\Delta w_f}^i + (\Pi_3)^{-1} * \Pi_2 Z_1$, therefore:

$$\overline{\Delta w_f}^i = \left(F_l' - (\Pi_3)^{-1} * \Pi_2\right) Z_1 + G_l' = F_l Z_1 + G_l$$

Thus the Theorem 1 is proved.

From theorem 2, we can see that controller designed for any partition is actually a state feedback control with a feed-forward filter.

Furthermore, the solution of Z_{10} in equation (18) is based on the method in reference [10], and with the help of Chebyshev distance, the following optimization problem is solved on any partition of Z_1 parameter space (here, it is assumed that the inequality corresponding to the partition is $\begin{matrix} -T_l Z_1 < -\theta_l \\ T_j Z_1 \le \theta_j, \forall j < l \end{matrix}$):

$$\begin{aligned} &\max_{Z_1, Z, \varepsilon} \ \varepsilon \\ &s.t.\ -T_l Z_1 < -\theta_l \\ &\quad T_j Z_1 \le \theta_j, \quad \forall j < l \\ &\quad GZ \le W + SZ_1 \end{aligned} \tag{20}$$

If $\varepsilon \le 0$, then the problem in equation (20) is infeasible for all Z_1 in this partition. Otherwise, we fix $Z_1 = Z_{10}$ and obtain Z_0 based on the following standard quadratic optimization problem:

$$\min_Z \frac{1}{2} Z^T H Z$$

$$\begin{aligned} &s.t.\ GZ \le W + SZ_1 \\ &\quad -T_l Z_1 < -\theta_l \\ &\quad T_j Z_1 \le \theta_j, \quad \forall j < l \end{aligned} \tag{21}$$

Finally, based on Lemma 1-2, the solutions Z_{10}, Z_0 of equations (20)-(21) and Theorem 2, the EMPC controller algorithm of turboshaft engine-rotor system is summarized in Table 2.

D. IMPLEMENTATION OF EMPC FAULT TOLERANT CONTROL ALGORITHM

After constructing EMPC controllers for models in the dynamic library off-line as stated above, the whole fault tolerant EMPC controller for turboshaft engine online implementation will be possible. The online control will require less amount of computation. During engine operation, the monitoring mechanism will decide which mode engine is working on. Within the mode provided from the monitoring mechanism, the controller module will decide the sub-model that best describes current engine dynamics. The offline decided EMPC controller designed for this sub-model will be activated. By querying which partition the current engine states fall in, the controller gain will be obtained. The controller output is now can be calculated with simple calculation with gain obtained. The whole procedure is shown in Fig.2.

TABLE 2. Algorithm 1: EMPC controller iteration algorithm.

Step 1: In the space $GZ \leqslant W + SZ_1$, based on the optimization problem (20), find the initial value of the parameter Z_{10};
Step 2: Fix Z_{10}, and obtain $\begin{bmatrix} Z_0 \\ \lambda_0 \end{bmatrix}$ by solving quadratic programming optimization problem equation (21);
Step 3: Determine the critical region ϑ_l near the equilibrium point $\begin{bmatrix} Z_0 \\ \lambda_0 \end{bmatrix}$ by judging whether λ_0 is greater than 0;
Step 4: Based on Equation (19) in Theorem 2 to obtain the expressions of $\begin{bmatrix} Z(Z_1) \\ \lambda(Z_1) \end{bmatrix}$ and $\Delta w_f(Z_1)$ in the critical region ϑ_l;
Step 5: Divide the critical region based on the method in reference [13] to obtain all the subcritical region of this critical region;
Step 6: Repeat the above steps to segment each subcritical domain iteratively, and determine the values of $\begin{bmatrix} Z(Z_1) \\ \lambda(Z_1) \end{bmatrix}$ and $\Delta w_f(Z_1)$ in each polyhedron (polyhedron) based on Theorem 2.

IV. SIMULATION VALIDATION OF EMPC FAULT TOLERANT CONTROLLER

A. VALIDATION OF FAULT MODEL LIBRARY

For the engine system under either normal mode or fault modes, 10 equilibrium points at the ground state are selected to establish PWA system for each mode to build the dynamic model library. Due to space limitation, the data of equilibrium points and PWA system are shown in Appendix A. The simulation results of component level models of PWA system and turboshaft engine rotor system are shown in Fig. 4-Fig. 7. Where:

1) Normal mode: PWA model under normal engine condition.

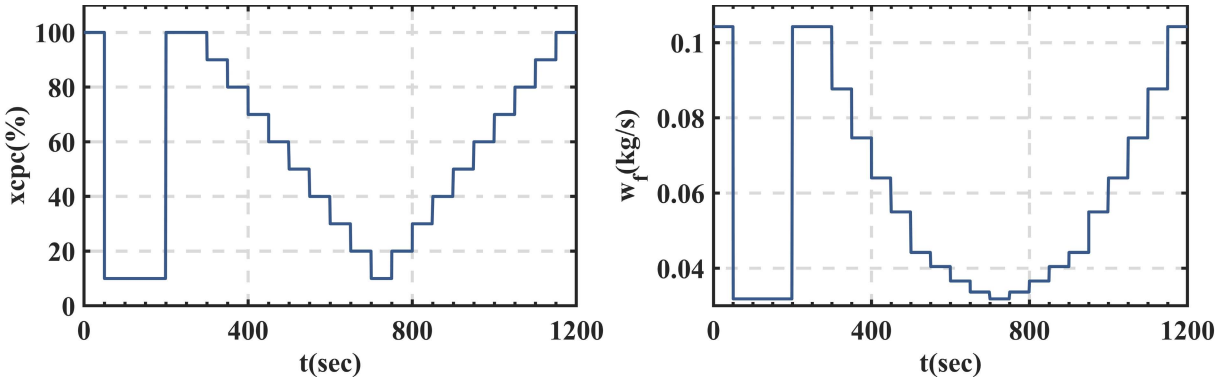

FIGURE 4. The step input signal of collective pitch *xcpc* and fuel flow w_f.

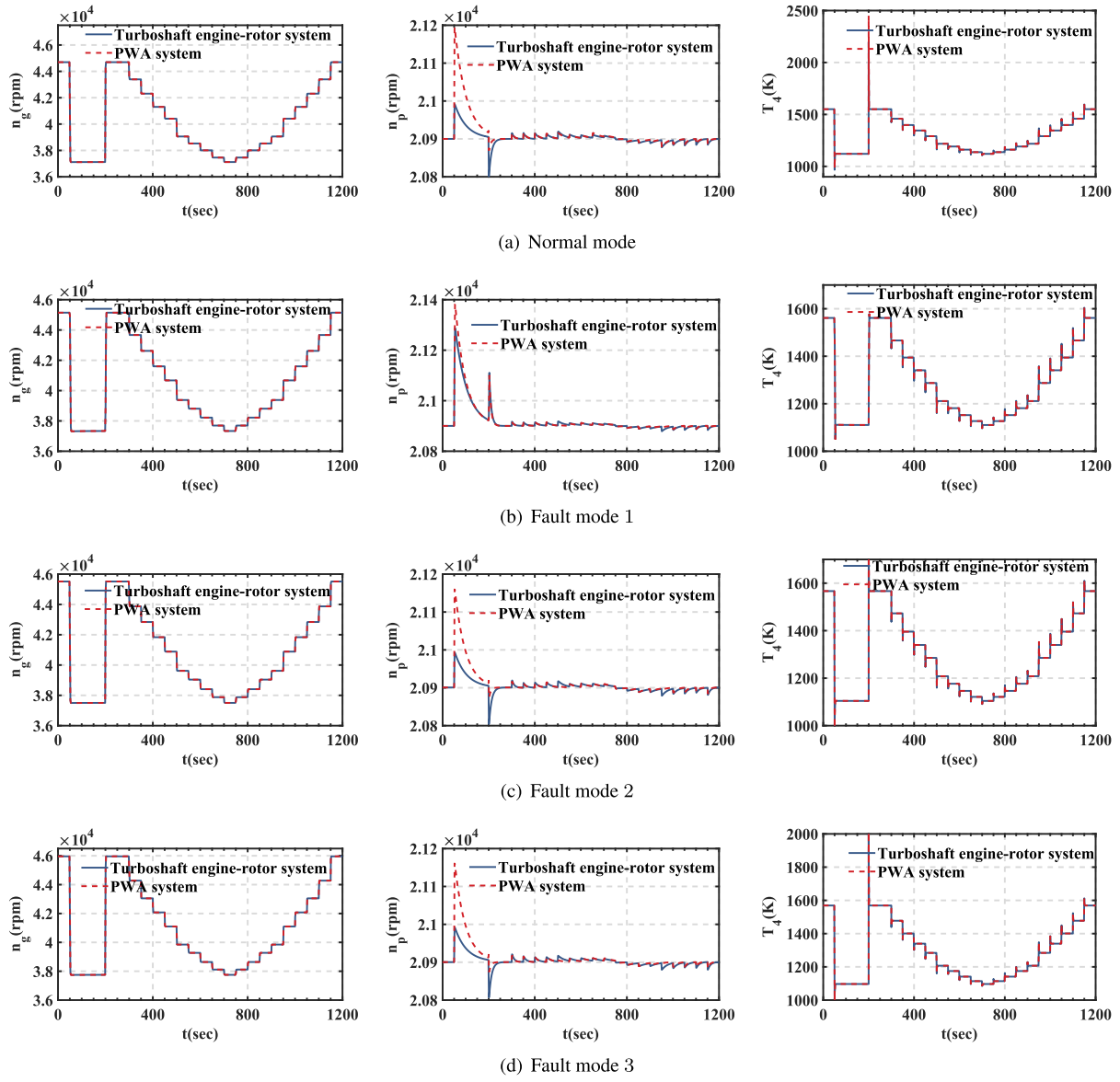

(a) Normal mode

(b) Fault mode 1

(c) Fault mode 2

(d) Fault mode 3

FIGURE 5. The step response curves of gas turbine speed n_g, power turbine speed n_p, and gas turbine inlet temperature T_4.

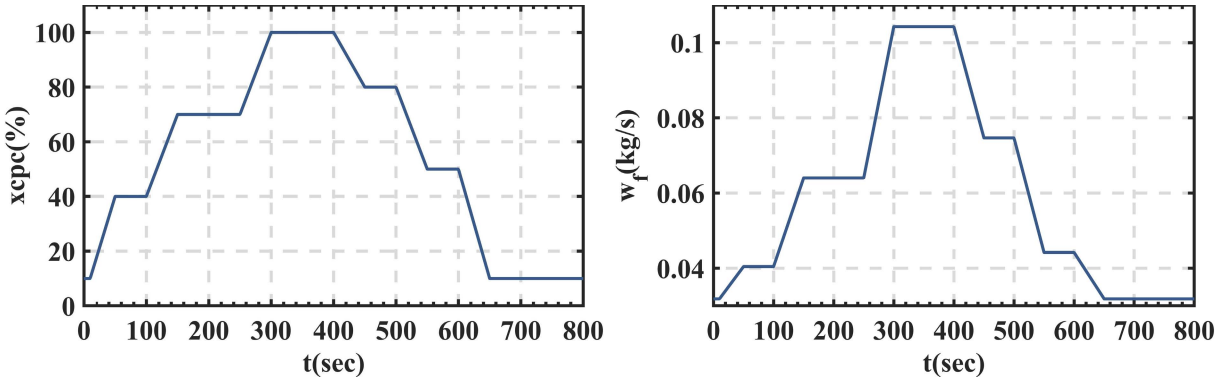

FIGURE 6. The ramp input signal of collective pitch *xcpc* and fuel flow w_f.

2) Fault mode 1: Fault PWA model when the compressor mass flow factor decays by 3%.
3) Fault mode 2: Fault PWA model when the compressor mass flow factor decays by 5%.
4) Fault mode 3: Fault PWA model when the compressor mass flow factor decays by 7%.

It can be seen from Fig. 5 and Fig.7 that the maximum steady-state and dynamic errors between PWA models and nonlinear model of the system speed response curve in normal mode and fault modes do not exceed 1% of the design point data. As for gas turbine inlet temperature, the errors are less than 1.5%, regardless of the step input signal or ramp input signal of the fuel w_f and the collective pitch *xcpc*. Therefore, the PWA system is basically consistent with the nonlinear model output of turboshaft engine rotor system. The established model library can meet the design requirements of the controller.

After completing the modeling of the turboshaft engine-rotor component-level nonlinear system and the modeling of the PWA system, the fault-tolerant control system can be constructed. The following section will discuss the effectiveness and robustness of the constructed EMPC fault tolerant controller under modeled and un-model faults.

B. FAULT TOLERANCE VERIFICATION OF KNOWN FAULTS

Under compressor faults(compressor mass flow factor degradation), the test simulation is proceeded by rapid step change of collective pitch input from 10% position to 100% of maximum position, as shown in Fig. 8. The control system shall have the ability to make the power turbine speed quickly track the command 20900(*rpm*), and ensure that the fuel flow w_f, gas turbine speed n_g and gas turbine inlet temperature T_4 all work within the set limit.

Assuming that the engine performance degrades at 90*s*, 140*s*, and 170*s*, the compressor flow factor drops from 1 to 0.97, 0.95 and 0.93, respectively. Whether in normal mode or fault mode, the controller performance weighted design parameter Q is set to 1, and the value of R is 0.5. See Table 3 for other parameter settings. The simulation results with and without fault tolerance control are shown in Fig. 9-Fig. 12.

Fig. 9 shows the decay curve of the compressor mass flow factor (9(a)) and the response curve of the monitoring mechanism (9(b)): state 1 indicates that the EMPC fault-tolerant controller is activated in the normal state. States 2, 3 and 4 represent that the EMPC controller is activated when the compressor mass flow factor is 0.97, 0.95 and 0.93 respectively. From the curve of the mass flow factor, it can be seen that the compressor fault occurs at 90*s* where the flow factor decreases from 1 to 0.97. The monitoring mechanism detects the fault in 90.19*s*, successfully switches to fault state 2, and starts the EMPC fault-tolerant controller designed for this fault mode. At 140*s*, the compressor experiences a further failure: the flow factor decays to 0.95, this degradation is detected by the monitoring mechanism at 140.24*s* and state 3 is correctly flagged which will switch control to the corresponding EMPC controller of this mode. Similar response can be observed when compressor mass flow factor decrease to 0.93. The longest time required to determine the fault does not exceed 0.27*s* when a fault occurs.

To see the necessity of including fault tolerant in the control procedure, we will compare the control performance of the controller with fault tolerant and the one without fault tolerant. The controller without fault tolerant is designed with a model library without engine models under fault modes. As under fault modes, engine dynamics will deviate from normal mode largely, the controller performance will decrease largely as discussed below.

Fig. 10 shows the fuel flow response curves under controllers with or without fault-tolerant. From the response curves of fuel flow w_f, it can be seen that whether the controller has fault-tolerant function or not, both controllers can ensure that the fuel flow works within the specified range. However, with fault tolerant, the control system will switch the controller according to the switching command based on the monitoring mechanism and automatically adjust the change of fuel flow to adapt to the impact of engine system degradation. As for controller without fault tolerant, the largely deviated dynamics caused by compressor fault will not be fully compensated by the fuel flow

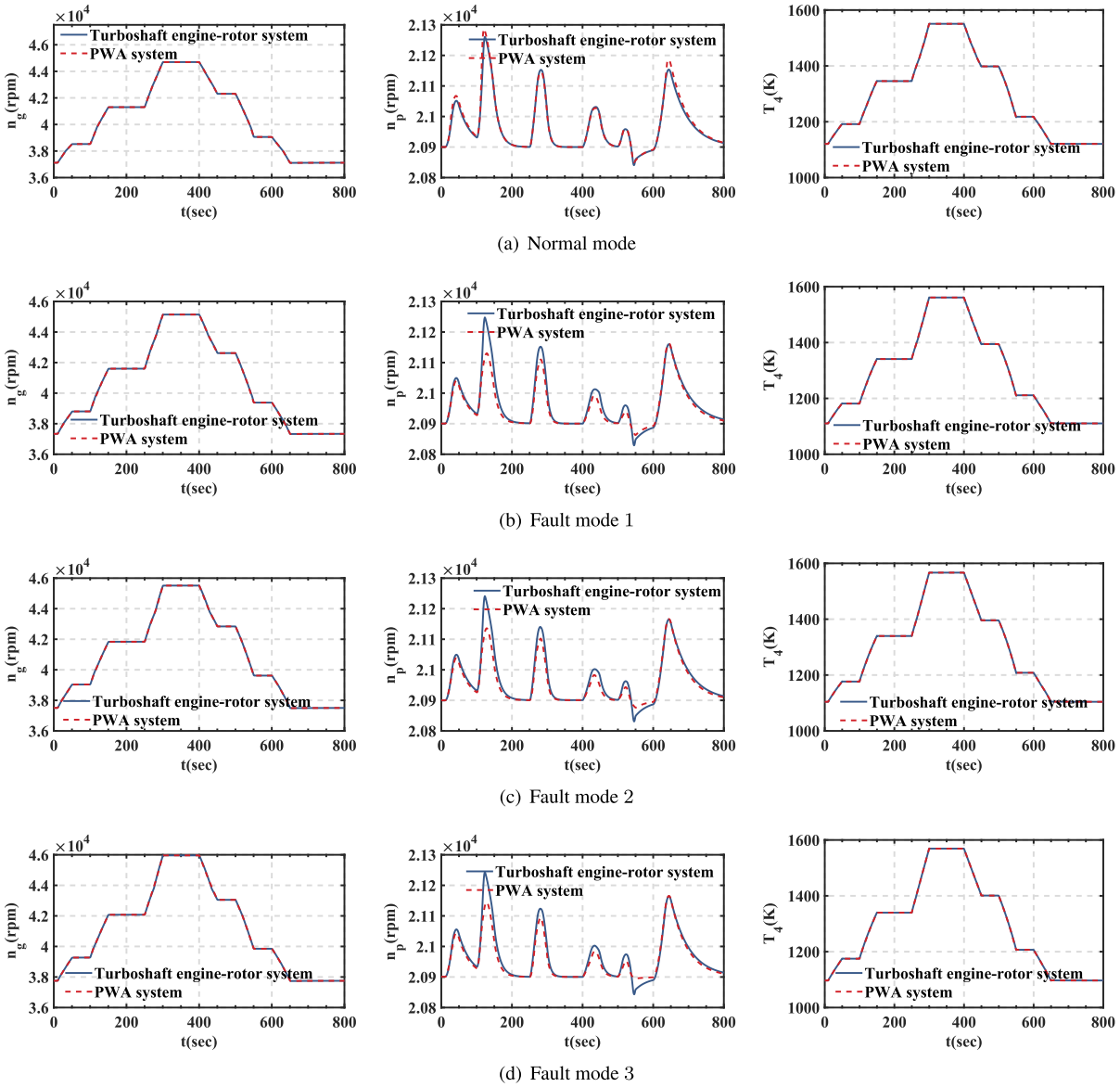

FIGURE 7. The ramp response curves of gas turbine speed n_g, power turbine speed n_p, and gas turbine inlet temperature T_4.

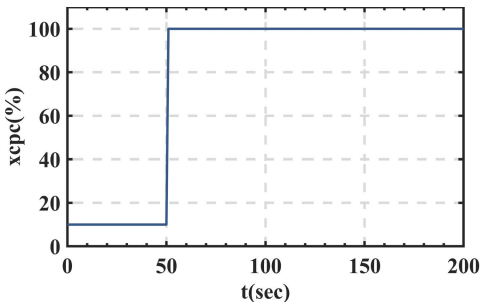

FIGURE 8. Step input signal of collective pitch *xcpc*.

provided by the controller. The mismatched fuel flow will lead to unsuccessful tracking of reference command as shown bellow.

TABLE 3. Simulation parameter table.

Symbol	Value
N_y	3
constraints	$w_f \leqslant 0.11(kg/s)$ $n_g \leqslant 47000(rpm)$ $T_4 \leq 1700(K)$

Fig. 11 is the response curves of gas turbine speed n_g and power turbine speed n_p. Among them, whether it is a controller with fault tolerant or without fault tolerant, it can ensure that the gas turbine speed is within a specified range. However, the controller without fault tolerance can not guarantee the good tracking performance of the power turbine speed. When the compressor exhibits performance degradation as shown in Fig. 9(a), the controller without fault

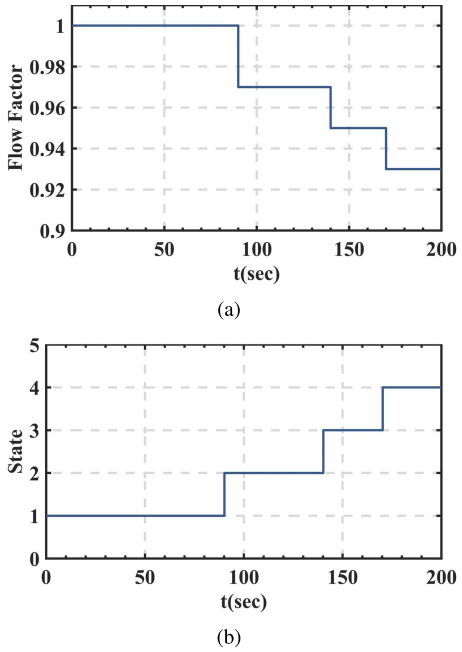

FIGURE 9. Compressor flow factor decay curve 9(a) and response curve of monitoring mechanism 9(b).

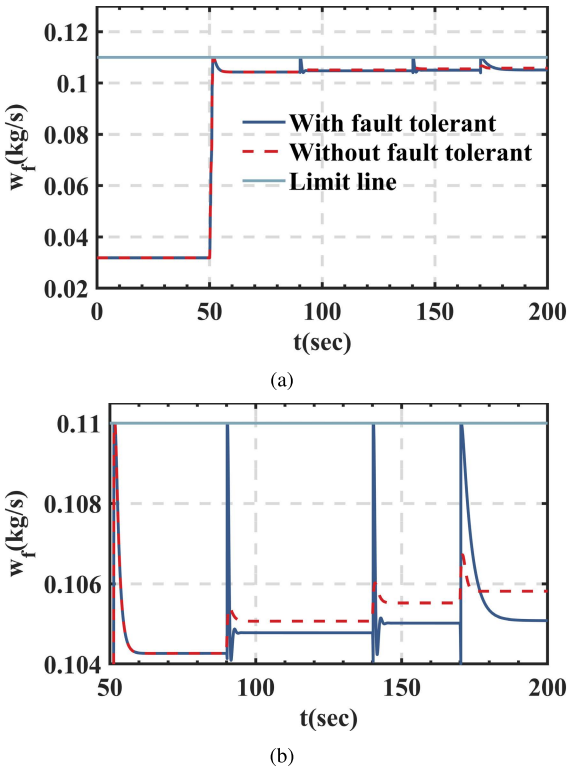

FIGURE 10. Response curves of fuel w_f 10(a) and its detailed diagram 10(b).

tolerance can not track power turbine speed reference command: the steady state error is too large. The fault-tolerant controller however, in the presence of compressor degradation, can still guarantee fast and stable tracking performance

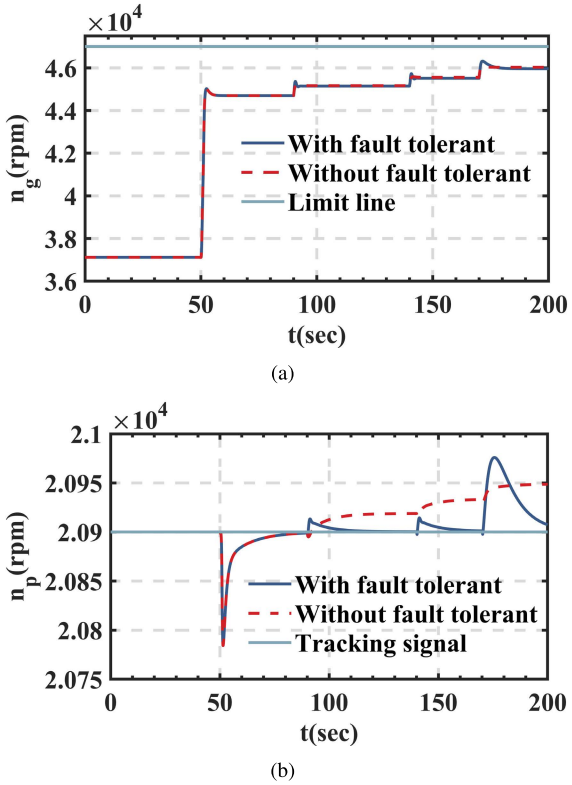

FIGURE 11. Response curves of fuel gas turbine n_g 11(a) and power turbine n_p 11(b).

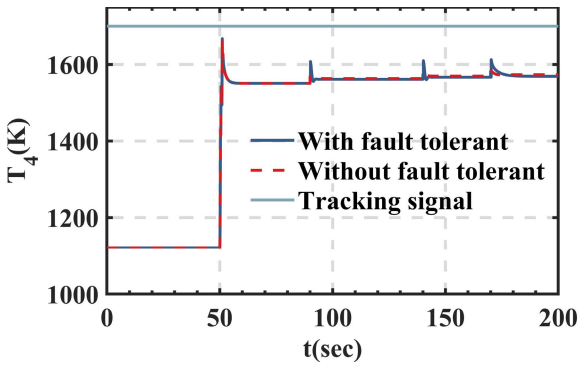

FIGURE 12. The response curve of gas turbine inlet temperature T_4.

of power turbine speed(steady-state error $< 0.05\%$ and maximum overshoot in the process of transition state $< 0.5\%$) which meets the needs of practical engineering. This further proves the effectiveness of the designed controller.

Fig. 12 shows the gas turbine inlet temperature response curves. The response and conclusion is similar to above discussion on turbine speed response.

Note4: The algorithm is universal and can ensure the limitation of other key parameters of engine section. For the limitation of different key parameters, it is only necessary to modify the parameter matrix C^i, D^i, D^i_w corresponding to the system output in equation (2), and convert it into the form

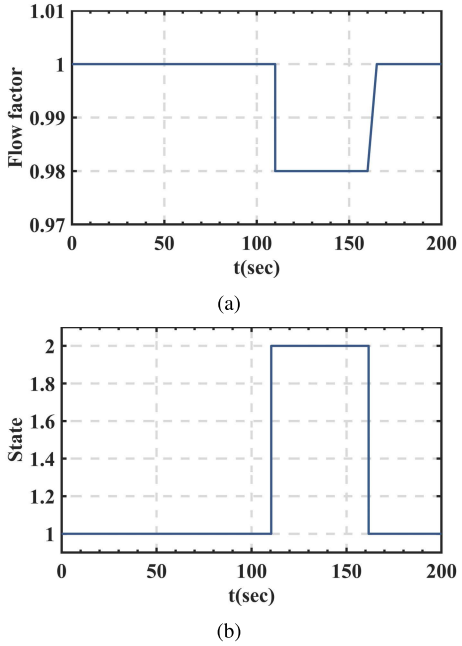

FIGURE 13. Compressor flow factor decay curve 13(a) and response curve of monitoring mechanism 13(b).

of (15) to complete the controller design according to the method in the proof of Theorem 1.

Note5: In order to verify the real-time performance of EMPC control algorithm, based on 3.4GHz Intel processor, simulation verification is carried out considering different length prediction time domain. The selection of N_y is shown in Table 4. In addition, the sampling time T_s is 0.01(sec) for simulation setting.

C. ROBUSTNESS VERIFICATION OF THE ALGORITHM

Furthermore, the robust fault-tolerant capability of the EMPC fault-tolerant controller designed in this paper is tested under scenario where un-modeled faults are introduced. Under such scenario engine dynamics deviate from modeled dynamics to a small scale. This is different from controller without fault tolerant where engine dynamics deviate largely from modeled dynamics. We will see that the designed controller is robust enough to handle such uncertainty. This robustness may stem from the fact that the EMPC controller on any partition is actually a state feedback controller as shown in equation (19). The following is detailed analysis.

We assume that the compressor inlet mass flow decreases temporarily first due to possible external objects block and resumes to normal value after a period of time. This fault is simulated by the change of mass flow factor as shown in Fig. 13(a). The mass flow factor decrease to 0.98 which has not been modeled in the engine model library. In the following section we will discuss how the proposed controller will react to such unmodeled faults. Other settings like collective pitch inputs and constrained parameters values are the same as above sections.

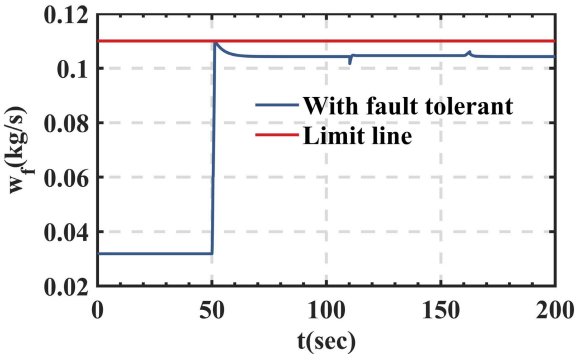

FIGURE 14. Response curves of fuel w_f under unknown fault.

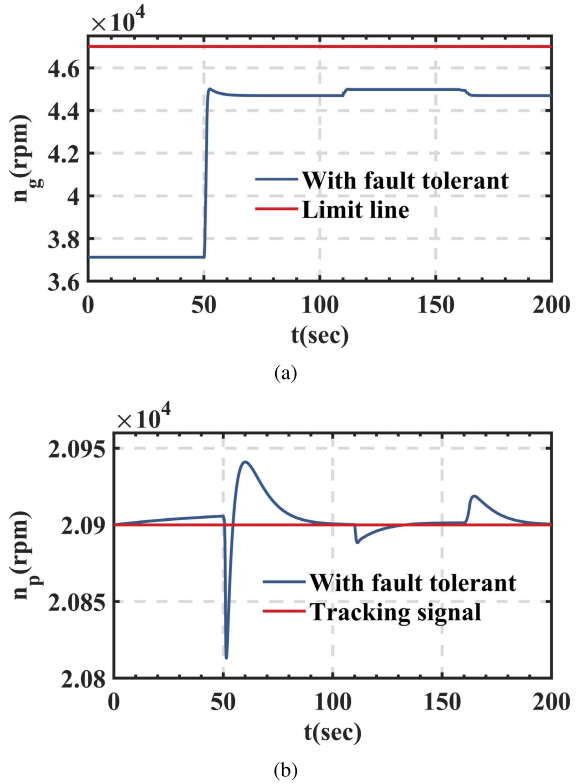

FIGURE 15. Response curves of gas turbine n_g 15(a) and power turbine n_p 15(b) under unknown fault.

Fig. 13(b) is the response curve of the monitoring mechanism under such test case. As a reminder, state 1 and 2 represents normal state and 0.97 mass flow factor mode respectively in monitoring mechanism.

As the figure shows, when the compressor mass flow factor decrease fault occurs, the monitoring mechanism detects the fault quickly and switches to state 2. This may be because that the engine dynamic of 0.98 mass flow factor is closer to 0.97 one. And after the engine return to normal mode, the monitoring mechanism change to state 1 correspondingly.

Figs 14-16 reflect the EMPC fault-tolerant controller performance under unmodeled faults through the response curves of fuel flow w_f, turbine speed (n_g, n_p) and gas turbine

TABLE 4. Real time verification table.

N_y	Partition number	Average computing time(sec)		Maximum computing time(sec)	
		EMPC	MPC	EMPC	MPC
3	225	7.8270e-4	0.4209	3.5050e-4	3.9680e-2
5	1557	7.9000e-4	0.4782	2.6660e-4	1.1966e-2
7	5892	9.1960e-4	0.5331	7.1950e-4	3.2030e-2
9	18888	8.0130e-4	0.5265	2.1990e-4	2.7146e-2

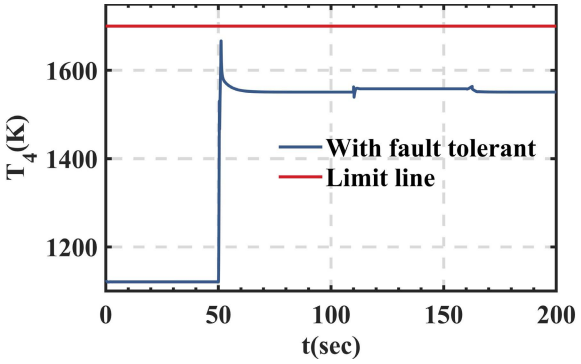

FIGURE 16. The response curve of gas turbine inlet temperature T_4 under unknown fault.

temperature T_4 : Firstly, in presence of unmodeled faults in the engine, EMPC fault-tolerant controller can still ensure the all constrained parameters work within the specified range without exceeding the limit. The power turbine speed n_p can be tracked according to the reference commands very well (steady-state error $<$ 0.05% and the maximum overshoot $<$ 0.5%), which can meet the needs of practical engineering.

Note6: For other engine faults, such as fuel system fault, actuator or sensor fault, lubricating oil system fault, etc., you can consider modeling the fault first and incorporate it into the algorithm as a kind of limitation.

V. CONCLUSION

Aiming at solving the problem of possible engine performance degradation faults and real time application difficulty of MPC algorithms, an EMPC fault-tolerant controller is designed in this paper. To verify the proposed controller design algorithm, compressor flow mass fault is used as examples. It is shown that under such compressor degradation test cases, the controller can provide good and stable engine power turbine speed tracking ability according to specified reference signal(steady-state error $<$ 0.05%) and can ensure the restriction requirements for key parameters in the process of engine transition state. At the same time, it has good dynamic response (maximum overshoot $<$ 0.9%). Fault tolerant capability is also achieved. The robustness of the algorithm and the effectiveness of fault control under unmodeled faults are verified by simulation. At present, the fault tolerance of EMPC controller performance test for other types of engine faults (actuator and sensor failures, etc.) has not been carried out, those can be treated in similar way as this paper described. Although the proposed EMPC algorithm is enough to guarantee real time performance for the turboshaft engine-rotor system, further improvement could be achieved according to suggestion in [20], [21] and could be an interesting future work.

APPENDIX A
PWA SYSTEM DATA SUPPLEMENT IN DYNAMIC MODEL LIBRARY

A. A1: PWA SYSTEM IN NORMAL MODE

In the case of $H = 0$, $Ma = 0$, 10 equilibrium points are selected to establish the PWA model for the turboshaft engine-rotor nonlinear system under normal conditions. Among them, some of the equilibrium point data are as follows:

1) equilibrium point 1($i = 1$): $xcpc = 100$, $[n_g\ n_p] = [44679.7259\ 20900]$

$$A^1 = \begin{bmatrix} 0.9665 & -0.0003 \\ 0.0009 & 0.9988 \end{bmatrix}$$
$$B^1 = \begin{bmatrix} 0.0061 \\ 0.0002 \end{bmatrix}$$
$$B_w^1 = \begin{bmatrix} 1.0258e-7 \\ -0.0006 \end{bmatrix}$$
$$C^1 = \begin{bmatrix} 1 & 0 \\ 0 & 1 \\ -0.7751 & 5.7379e-5 \end{bmatrix}$$
$$D^1 = \begin{bmatrix} 0 \\ 0 \\ 0.5157 \end{bmatrix}, \quad D_w^1 = \begin{bmatrix} 0 \\ 0 \\ 0 \end{bmatrix} \tag{22}$$

2) equilibrium point 2($i = 2$): $xcpc = 90$, $[n_g\ n_p] = [43393.4576\ 20900]$

$$A^2 = \begin{bmatrix} 0.9641 & -0.0003 \\ 0.0011 & 0.9990 \end{bmatrix}$$
$$B^2 = \begin{bmatrix} 0.0066 \\ 0.0002 \end{bmatrix}$$
$$B_w^2 = \begin{bmatrix} 8.8320e-8 \\ -0.0006 \end{bmatrix}$$
$$C^2 = \begin{bmatrix} 1 & 0 \\ 0 & 1 \\ -0.7105 & 3.3732e-5 \end{bmatrix}$$
$$D^2 = \begin{bmatrix} 0 \\ 0 \\ 0.5220 \end{bmatrix}, \quad D_w^2 = \begin{bmatrix} 0 \\ 0 \\ 0 \end{bmatrix} \tag{23}$$

3) equilibrium point 3($i = 6$): $xcpc = 50$, $[n_g\ n_p] = [39059.0789\ 20900]$

$$A^6 = \begin{bmatrix} 0.9803 & -0.0004 \\ 0.0007 & 0.9997 \end{bmatrix}$$
$$B^6 = \begin{bmatrix} 0.0069 \\ 0.0002 \end{bmatrix}$$
$$B_w^6 = \begin{bmatrix} 2.8358e-8 \\ -0.0002 \end{bmatrix}$$
$$C^6 = \begin{bmatrix} 1 & 0 \\ 0 & 1 \\ -1.3490 & 9.0893e-5 \end{bmatrix}$$
$$D^6 = \begin{bmatrix} 0 \\ 0 \\ 0.9415 \end{bmatrix}, \quad D_w^6 = \begin{bmatrix} 0 \\ 0 \\ 0 \end{bmatrix} \tag{24}$$

4) equilibrium point 4($i = 8$): $xcpc = 30$, $[n_g\ n_p] = [38007.2583\ 20900]$

$$A^8 = \begin{bmatrix} 0.9807 & -0.0003 \\ 0.0007 & 0.9998 \end{bmatrix}$$
$$B^8 = \begin{bmatrix} 0.0075 \\ 0.0002 \end{bmatrix}$$
$$B_w^8 = \begin{bmatrix} 2.5422e-8 \\ -0.0001 \end{bmatrix}$$
$$C^8 = \begin{bmatrix} 1 & 0 \\ 0 & 1 \\ -1.5015 & 0.0001 \end{bmatrix}$$
$$D^8 = \begin{bmatrix} 0 \\ 0 \\ 1.1199 \end{bmatrix}, \quad D_w^8 = \begin{bmatrix} 0 \\ 0 \\ 0 \end{bmatrix} \tag{25}$$

5) equilibrium point 5($i = 10$): $xcpc = 10$, $[n_g\ n_p] = [37119.1035\ 20900]$

$$A^{10} = \begin{bmatrix} 0.9820 & -0.0004 \\ 0.0005 & 0.9998 \end{bmatrix}$$
$$B^{10} = \begin{bmatrix} 0.0078 \\ 0.0001 \end{bmatrix}$$
$$B_w^{10} = \begin{bmatrix} 1.4611e-8 \\ -6.6602e-5 \end{bmatrix}$$
$$C^{10} = \begin{bmatrix} 1 & 0 \\ 0 & 1 \\ -1.3994 & 0.0001 \end{bmatrix}$$
$$D^{10} = \begin{bmatrix} 0 \\ 0 \\ 1.2339 \end{bmatrix}, \quad D_w^{10} = \begin{bmatrix} 0 \\ 0 \\ 0 \end{bmatrix} \tag{26}$$

B. A2: FAULT PWA MODEL WHEN THE COMPRESSOR FLOW FACTOR DECAYS BY 3%

In the case of $H = 0$, $Ma = 0$, 10 equilibrium points are selected to establish the fault PWA model for the turboshaft engine-rotor nonlinear system when the compressor flow factor decays by 3%. Among them, some of the equilibrium point data are as follows:

1) equilibrium point 1($i = 1$): $xcpc = 100$, $[n_g\ n_p] = [45144.3315\ 20900]$

$$A^1 = \begin{bmatrix} 0.9609 & -3.9797e-4 \\ 5.1910e-4 & 0.9987 \end{bmatrix}$$
$$B^1 = \begin{bmatrix} 0.0056 \\ 2.3906e-4 \end{bmatrix}$$
$$B_w^1 = \begin{bmatrix} 1.2642e-7 \\ -6.3148e-4 \end{bmatrix}$$
$$C^1 = \begin{bmatrix} 1 & 0 \\ 0 & 1 \\ -0.6956 & 1.9017e-5 \end{bmatrix}$$
$$D^1 = \begin{bmatrix} 0 \\ 0 \\ 0.5086 \end{bmatrix}, \quad D_w^1 = \begin{bmatrix} 0 \\ 0 \\ 0 \end{bmatrix} \tag{27}$$

2) equilibrium point 2($i = 2$): $xcpc = 90$, $[n_g\ n_p] = [43669.7396\ 20900]$

$$A^2 = \begin{bmatrix} 0.9599 & -4.0337e-4 \\ 0.0011 & 0.9989 \end{bmatrix}$$
$$B^2 = \begin{bmatrix} 0.0068 \\ 2.1469e-4 \end{bmatrix}$$
$$B_w^2 = \begin{bmatrix} 1.2642e-7 \\ -6.3148e-4 \end{bmatrix}$$
$$C^2 = \begin{bmatrix} 1 & 0 \\ 0 & 1 \\ -1.2289 & 3.1530e-5 \end{bmatrix}$$
$$D^2 = \begin{bmatrix} 0 \\ 0 \\ 0.5596 \end{bmatrix}, \quad D_w^2 = \begin{bmatrix} 0 \\ 0 \\ 0 \end{bmatrix} \tag{28}$$

3) equilibrium point 3($i = 6$): $xcpc = 50$, $[n_g\ n_p] = [39379.4722\ 20900]$

$$A^6 = \begin{bmatrix} 0.9810 & -3.6322e-4 \\ 6.6567e-4 & 0.9997 \end{bmatrix}$$
$$B^6 = \begin{bmatrix} 0.0065 \\ 2.0784e-4 \end{bmatrix}$$
$$B_w^6 = \begin{bmatrix} 2.8668e-8 \\ -1.5732e-4 \end{bmatrix}$$
$$C^6 = \begin{bmatrix} 1 & 0 \\ 0 & 1 \\ -1.1588 & 6.5405e-5 \end{bmatrix}$$
$$D^6 = \begin{bmatrix} 0 \\ 0 \\ 0.0.8998 \end{bmatrix}, \quad D_w^6 = \begin{bmatrix} 0 \\ 0 \\ 0 \end{bmatrix} \tag{29}$$

4) equilibrium point 4($i = 8$): $xcpc = 30$, $[n_g\ n_p] = [38218.1875\ 20900]$

$$A^8 = \begin{bmatrix} 0.9800 & -3.5778e-4 \\ 7.0478e-4 & 0.9998 \end{bmatrix}$$
$$B^8 = \begin{bmatrix} 0.0071 \\ 1.7775e-4 \end{bmatrix}$$

$$B_w^8 = \begin{bmatrix} 2.7517e-8 \\ -1.5328e-4 \end{bmatrix}$$
$$C^8 = \begin{bmatrix} 1 & 0 \\ 0 & 1 \\ -1.4251 & 0.0001 \end{bmatrix}$$
$$D^8 = \begin{bmatrix} 0 \\ 0 \\ 1.0597 \end{bmatrix}, \quad D_w^8 = \begin{bmatrix} 0 \\ 0 \\ 0 \end{bmatrix} \tag{30}$$

5) equilibrium point 5($i = 10$): $xcpc = 10$, $\begin{bmatrix} n_g & n_p \end{bmatrix} = \begin{bmatrix} 37335.0997 & 20900 \end{bmatrix}$

$$A^{10} = \begin{bmatrix} 0.9833 & -4.2095e-4 \\ 4.8366e-4 & 0.9998 \end{bmatrix}$$
$$B^{10} = \begin{bmatrix} 0.0076 \\ 1.4957e-4 \end{bmatrix}$$
$$B_w^{10} = \begin{bmatrix} 1.7294e-8 \\ -8.1927e-5 \end{bmatrix}$$
$$C^{10} = \begin{bmatrix} 1 & 0 \\ 0 & 1 \\ -1.2520 & 0.0001 \end{bmatrix}$$
$$D^{10} = \begin{bmatrix} 0 \\ 0 \\ 1.2036 \end{bmatrix}, \quad D_w^{10} = \begin{bmatrix} 0 \\ 0 \\ 0 \end{bmatrix} \tag{31}$$

C. A3: FAULT PWA MODEL WHEN THE COMPRESSOR FLOW FACTOR DECAYS BY 5%

In the case of $H = 0$, $Ma = 0$, 10 equilibrium points are selected to establish the fault PWA model for the turboshaft engine-rotor nonlinear system when the compressor flow factor decays by 5%. Among them, some of the equilibrium point data are as follows:

1) equilibrium point 1($i = 1$): $xcpc = 100$, $\begin{bmatrix} n_g & n_p \end{bmatrix} = \begin{bmatrix} 45512.5344 & 20900 \end{bmatrix}$

$$A^1 = \begin{bmatrix} 0.9727 & -3.7917e-4 \\ 5.1729e-4 & 0.9987 \end{bmatrix}$$
$$B^1 = \begin{bmatrix} 0.0053 \\ 2.4351e-4 \end{bmatrix}$$
$$B_w^1 = \begin{bmatrix} 1.2038e-7 \\ -6.3149e-4 \end{bmatrix}$$
$$C^1 = \begin{bmatrix} 1 & 0 \\ 0 & 1 \\ -0.6908 & 2.0246e-5 \end{bmatrix}$$
$$D^1 = \begin{bmatrix} 0 \\ 0 \\ 0.5091 \end{bmatrix}, \quad D_w^1 = \begin{bmatrix} 0 \\ 0 \\ 0 \end{bmatrix} \tag{32}$$

2) equilibrium point 2($i = 2$): $xcpc = 90$, $\begin{bmatrix} n_g & n_p \end{bmatrix} = \begin{bmatrix} 43872.6171 & 20900 \end{bmatrix}$

$$A^2 = \begin{bmatrix} 0.9755 & -2.7516e-4 \\ 0.0011 & 0.9989 \end{bmatrix}$$
$$B^2 = \begin{bmatrix} 0.0064 \\ 2.2338e-4 \end{bmatrix}$$
$$B_w^2 = \begin{bmatrix} 8.0014e-8 \\ -5.7874e-4 \end{bmatrix}$$
$$C^2 = \begin{bmatrix} 1 & 0 \\ 0 & 1 \\ -0.6670 & 2.0476e-5 \end{bmatrix}$$
$$D^2 = \begin{bmatrix} 0 \\ 0 \\ 0.5536 \end{bmatrix}, \quad D_w^2 = \begin{bmatrix} 0 \\ 0 \\ 0 \end{bmatrix} \tag{33}$$

3) equilibrium point 3($i = 6$): $xcpc = 50$, $\begin{bmatrix} n_g & n_p \end{bmatrix} = \begin{bmatrix} 39618.5326 & 20900 \end{bmatrix}$

$$A^6 = \begin{bmatrix} 0.9811 & -3.5827e-4 \\ 6.6257e-4 & 0.9997 \end{bmatrix}$$
$$B^6 = \begin{bmatrix} 0.0065 \\ 2.0858e-4 \end{bmatrix}$$
$$B_w^6 = \begin{bmatrix} 2.8276e-8 \\ -1.5731e-4 \end{bmatrix}$$
$$C^6 = \begin{bmatrix} 1 & 0 \\ 0 & 1 \\ -1.1083 & 6.6019e-5 \end{bmatrix}$$
$$D^6 = \begin{bmatrix} 0 \\ 0 \\ 0.8943 \end{bmatrix}, \quad D_w^6 = \begin{bmatrix} 0 \\ 0 \\ 0 \end{bmatrix} \tag{34}$$

4) equilibrium point 4($i = 8$): $xcpc = 30$, $\begin{bmatrix} n_g & n_p \end{bmatrix} = \begin{bmatrix} 38406.2739 & 20900 \end{bmatrix}$

$$A^8 = \begin{bmatrix} 0.9826 & -3.2370e-4 \\ 7.0429e-4 & 0.9998 \end{bmatrix}$$
$$B^8 = \begin{bmatrix} 0.0069 \\ 1.8316e-4 \end{bmatrix}$$
$$B_w^8 = \begin{bmatrix} 2.4886e-8 \\ -1.5329e-4 \end{bmatrix}$$
$$C^8 = \begin{bmatrix} 1 & 0 \\ 0 & 1 \\ -1.2786 & 9.7758e-5 \end{bmatrix}$$
$$D^8 = \begin{bmatrix} 0 \\ 0 \\ 1.0445 \end{bmatrix}, \quad D_w^8 = \begin{bmatrix} 0 \\ 0 \\ 0 \end{bmatrix} \tag{35}$$

5) equilibrium point 5($i = 10$): $xcpc = 10$, $\begin{bmatrix} n_g & n_p \end{bmatrix} = \begin{bmatrix} 37502.8421 & 20900 \end{bmatrix}$

$$A^{10} = \begin{bmatrix} 0.9843 & -3.9619e-4 \\ 4.8316e-4 & 0.9998 \end{bmatrix}$$
$$B^{10} = \begin{bmatrix} 0.0075 \\ 1.5293e-4 \end{bmatrix}$$
$$B_w^{10} = \begin{bmatrix} 1.6215e-8 \\ -8.1630e-5 \end{bmatrix}$$
$$C^{10} = \begin{bmatrix} 1 & 0 \\ 0 & 1 \\ -1.1423 & 0.0001 \end{bmatrix}$$
$$D^{10} = \begin{bmatrix} 0 \\ 0 \\ 1.1890 \end{bmatrix}, \quad D_w^{10} = \begin{bmatrix} 0 \\ 0 \\ 0 \end{bmatrix} \tag{36}$$

D. A4: FAULT PWA MODEL WHEN THE COMPRESSOR FLOW FACTOR DECAYS BY 7%

In the case of $H = 0$, $Ma = 0$, 10 equilibrium points are selected to establish the fault PWA model for the turboshaft engine-rotor nonlinear system when the compressor flow factor decays by 7%. Among them, some of the equilibrium point data are as follows:

1) equilibrium point 1($i = 1$): $xcpc = 100$, $[n_g\ n_p] = [45960.6185\ 20900]$

$$A^1 = \begin{bmatrix} 0.9766 & -3.5949e-4 \\ 5.1565e-4 & 0.9987 \end{bmatrix}$$
$$B^1 = \begin{bmatrix} 0.0046 \\ 2.5074e-4 \end{bmatrix}$$
$$B_w^1 = \begin{bmatrix} 1.1405e-7 \\ -6.3148e-4 \end{bmatrix}$$
$$C^1 = \begin{bmatrix} 1 & 0 \\ 0 & 1 \\ -0.6870 & 2.2098e-5 \end{bmatrix}$$
$$D^1 = \begin{bmatrix} 0 \\ 0 \\ 0.5140 \end{bmatrix}, \quad D_w^1 = \begin{bmatrix} 0 \\ 0 \\ 0 \end{bmatrix} \tag{37}$$

2) equilibrium point 2($i = 2$): $xcpc = 90$, $[n_g\ n_p] = [44276.5526\ 20900]$

$$A^2 = \begin{bmatrix} 0.9783 & -2.6837e-4 \\ 0.0011 & 0.9989 \end{bmatrix}$$
$$B^2 = \begin{bmatrix} 0.0057 \\ 2.3384e-4 \end{bmatrix}$$
$$B_w^2 = \begin{bmatrix} 7.8009e-8 \\ -5.7880e-4 \end{bmatrix}$$
$$C^2 = \begin{bmatrix} 1 & 0 \\ 0 & 1 \\ -0.7022 & 2.6047e-5 \end{bmatrix}$$
$$D^2 = \begin{bmatrix} 0 \\ 0 \\ 0.5516 \end{bmatrix}, \quad D_w^2 = \begin{bmatrix} 0 \\ 0 \\ 0 \end{bmatrix} \tag{38}$$

3) equilibrium point 3($i = 6$): $xcpc = 50$, $[n_g\ n_p] = [39848.7379\ 20900]$

$$A^6 = \begin{bmatrix} 0.9742 & -4.3605e-4 \\ 6.5768e-4 & 0.9997 \end{bmatrix}$$
$$B^6 = \begin{bmatrix} 0.0068 \\ 2.1166e-4 \end{bmatrix}$$
$$B_w^6 = \begin{bmatrix} 3.4458e-8 \\ -1.5732e-4 \end{bmatrix}$$
$$C^6 = \begin{bmatrix} 1 & 0 \\ 0 & 1 \\ -1.2858 & 5.0311e-5 \end{bmatrix}$$
$$D^6 = \begin{bmatrix} 0 \\ 0 \\ 0.8725 \end{bmatrix}, \quad D_w^6 = \begin{bmatrix} 0 \\ 0 \\ 0 \end{bmatrix} \tag{39}$$

4) equilibrium point 4($i = 8$): $xcpc = 30$, $[n_g\ n_p] = [38639.0990\ 20900]$

$$A^8 = \begin{bmatrix} 0.9834 & -2.9756e-4 \\ 7.0228e-4 & 0.9998 \end{bmatrix}$$
$$B^8 = \begin{bmatrix} 0.0067 \\ 1.9227e-4 \end{bmatrix}$$
$$B_w^8 = \begin{bmatrix} 2.2873e-8 \\ -1.5329e-4 \end{bmatrix}$$
$$C^8 = \begin{bmatrix} 1 & 0 \\ 0 & 1 \\ -1.1069 & 7.5704e-5 \end{bmatrix}$$
$$D^8 = \begin{bmatrix} 0 \\ 0 \\ 1.0107 \end{bmatrix}, \quad D_w^8 = \begin{bmatrix} 0 \\ 0 \\ 0 \end{bmatrix} \tag{40}$$

5) equilibrium point 5($i = 10$): $xcpc = 10$, $[n_g\ n_p] = [37751.05196\ 20900]$

$$A^{10} = \begin{bmatrix} 0.9870 & -3.4934e-4 \\ 4.8340e-4 & 0.9998 \end{bmatrix}$$
$$B^{10} = \begin{bmatrix} 0.0065 \\ 1.7495e-4 \end{bmatrix}$$
$$B_w^{10} = \begin{bmatrix} 1.4343e-8 \\ -8.1928e-5 \end{bmatrix}]$$
$$C^{10} = \begin{bmatrix} 1 & 0 \\ 0 & 1 \\ -1.0073 & 0.0001 \end{bmatrix}$$
$$D^{10} = \begin{bmatrix} 0 \\ 0 \\ 1.1373 \end{bmatrix}, \quad D_w^{10} = \begin{bmatrix} 0 \\ 0 \\ 0 \end{bmatrix} \tag{41}$$

APPENDIX B
DATA SUPPLEMENT OF THEOREM 1

$$P_x^i = \begin{bmatrix} A \\ \vdots \\ A^{N_y} \end{bmatrix} \tag{42}$$

$$P_u^i = \begin{bmatrix} B^i & 0 & \cdots & 0 \\ A^iB^i & B^i & \cdots & 0 \\ \vdots & \vdots & \ddots & \vdots \\ A^{N_y-1}B^i & A^{N_y-2}B^i & \cdots & B^i \end{bmatrix} \tag{43}$$

$$P_w^i = \begin{bmatrix} B_w^i & 0 & \cdots & 0 \\ A^iB_w^i & B_w^i & \cdots & 0 \\ \vdots & \vdots & \ddots & \vdots \\ A^{N_y-1}B_w^i & A^{N_y-2}B_w^i & \cdots & B_w^i \end{bmatrix} \tag{44}$$

$$P_{yx}^i = \begin{bmatrix} C^iA \\ \vdots \\ C^iA^{N_y} \end{bmatrix} \tag{45}$$

$$P^i_{yw} = \begin{bmatrix} C^iB^i_w & 0 & \cdots & 0 \\ C^iA^iB^i_w & C^iB^i_w & \cdots & 0 \\ \vdots & \vdots & \ddots & \vdots \\ C^iA^{N_y-1}B^i_w & C^iA^{N_y-2}B^i_w & \cdots & C^iB^i_w \end{bmatrix} \tag{46}$$

$$P^i_{yu} = \begin{bmatrix} C^iB^i & 0 & \cdots & 0 \\ C^iA^iB^i & C^iB^i & \cdots & 0 \\ \vdots & \vdots & \ddots & \vdots \\ C^iA^{N_y-1}B^i & C^iA^{N_y-2}B^i & \cdots & C^iB^i. \end{bmatrix} \tag{47}$$

REFERENCES

[1] H. BRasmussen, *Advanced Control of Turbofan Engines*. New York, NY, USA: Springer, 2012, pp. 100–223.

[2] M. G. Ballin, *A High Fidelity Real-Time Simulation of a Small Turboshaft Engine*. Washington DC, USA: NASA Technical Memorandum, 1988, pp. 15–69.

[3] T. Samad, S. Mastellone, P. Goupil, A. van Delft, A. Serbezov, and K. Brooks, "IFAC industry committee update, initiative to increase industrial participation in the control community," in *Newsletters April 2019*. New York, NY, USA: IFAC, 2019.

[4] X. Luo, T. Yang, and X. Jun, "Online optimization implementation on model predictive control in chemical process," *Ciesc J.*, vol. 65, no. 10, pp. 3984–3992, May 2014.

[5] Y. Yang and B. Ding, "Two–layer model predictive control for chemical process model with integrating controlled variables," *Can J. Chem. Eng.*, vol. 98, no. 1, pp. 237–253, Jul. 2019.

[6] X. Du, X. Sun, Z. Wang, and A. Dai, "A scheduling scheme of linear model predictive controllers for turbofan engines," *IEEE Access*, vol. 5, pp. 24533–24541, 2017.

[7] K. Ghanbarpour, F. Bayat, and A. Jalilvand, "Dependable power extraction in wind turbines using model predictive fault tolerant control," *Int. J. Electr. Power Energy Syst.*, vol. 118, pp. 1–22, 2020.

[8] A. Taherkhani, F. Bayat, S. Mobayen, and A. Bartoszewicz, "Dependable sensor fault reconstruction in air-path system of heavy-duty diesel engines," *Sensors*, vol. 21, pp. 1–13, Aug. 2021.

[9] W. Liu, G. Chen, and A. Knoll, "Matrix inequalities based robust model predictive control for vehicle considering model uncertainties, external disturbances, and time-varying delay," *Frontiers Neurorobot.*, vol. 14, pp. 1–8, Jan. 2021.

[10] P. Mhaskar, "Robust model predictive control design for fault-tolerant control of process systems," *IEC Res.*, vol. 45, no. 25, pp. 8565–8574, May 2006.

[11] J. M. Maciejowski and C. N. Jones, "MPC fault-tolerant flight control case study: Flight 1862," *IFAC Proc. Vol.*, vol. 36, no. 5, pp. 119–124, Jun. 2003.

[12] D. Saluru and R. Yedavalli, "Fault tolerant model predictive control of a turbofan engine using C-MAPSS40k," in *Proc. Aerosp. Sci. Meeting New Horizons Forum Aerosp. Expo.*, Jan. 2013, pp. 1–11.

[13] A. Bemporad, "The explicit solution of model predictive control via multiparametric quadratic programming," in *Proc. ACC*, Chicago, IL, USA, 2000, pp. 872–876.

[14] S. Verlag, *Advances in Sensitivity Analysis and Parametric Programming*. Norwell, MA, USA: Kluwer, 1988, pp. 4–45.

[15] J. Acevedo and E. Pistikopoulos, "A multiparametric programming approach for linear process engineering problems under uncertainty," *Ind. Eng. Chem. Res.*, vol. 36, no. 3, pp. 717–728, Mar. 1997.

[16] S. Hovland and K. E. Willcox, "Explicit model predictive control for large-scale systems via model reduction," *J. Guid. Control Dyn.*, vol. 31, no. 4, pp. 918–926, May 2012.

[17] S. Mariethoz, A. Domahidi, and M. Morari, "High-bandwidth explicit model predictive control of electrical drives," *IEEE Trans. Ind. Appl.*, vol. 48, no. 6, pp. 1980–1992, Oct. 2012.

[18] Z. J. Wang, "Explicit model predictive control for large inertia servo system," *J. Inst. Technol.*, vol. 31, no. 11, pp. 1307–1312, Nov. 2011.

[19] R. Kurz and K. Brun, "Degradation in gas turbine systems," *J. Eng. Gas Turbines Power*, vol. 123, no. 1, pp. 70–77, Nov. 2001.

[20] F. Bayat and T. A. Johansen, "Using hash tables to manage the time-storage complexity in a point location problem: Application to explicit model predictive control," *Automatica*, vol. 47, no. 3, pp. 571–577, 2011.

[21] F. Bayat and T. A. Johansen, "Flexible piecewise function evaluation methods based on truncated binary search trees and lattice representation in explicit MPC," *IEEE Trans. Control Syst. Technol.*, vol. 20, no. 3, pp. 632–640, May 2012.

NANNAN GU was born in Jining, Shandong. She received the bachelor's degree in information and computing science from Shandong Jianzhu University, in 2011, and the master's degree in operations research and cybernetics from Hebei Yanshan University, in 2014. She is currently pursuing the Ph.D. degree in energy and power engineering with the Beijing University of Aeronautics and Astronautics. So far, she has gained academic experience in four SCI papers, one EI paper, one international conference, and many domestic conferences. At the same time, she has independently undertaken and completed a National Natural Science Fund and a Key Research Project of Aviation Research Institute. Her current research interests include the modeling of the overall dynamic mathematical aero-engines, the design on the control system of the turboshaft-rotor systems, the design on the predictive control law of aero-engine model, and the fault tolerant design.

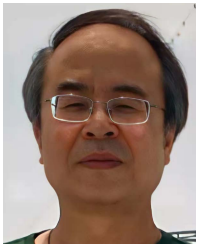

XI WANG was born in Shanxi. He received the Ph.D. degree from Northwestern Polytechnical University, in 1998. Currently, he is a Professor of energy and power engineering with Beihang University and a member of the basic research group of two major aircraft projects. He is also an Expert of two engines major special projects of the Third Research Institute of China Aerospace Science and Industry Corporation; a Specialized Expert of the Control and Health Management Group of Aerospace Power Technology Group; a member of the Automatic Control Professional Committee, Chinese Society of Aeronautics and Astronautics; a member of the China Aerospace No.3 Network Engine Control Specialty Committee; a member of Aerospace Power Control Technology Key Laboratory, Aero Engine Corporation of China; a Special Expert of the High-Altitude Simulation Technology Key Laboratory; a Doctoral Dissertation Evaluation Expert of the Degree Center, Ministry of Education. His research achievements are as follows: nine national patents for invention, 150 papers published in core journals and international conferences (ten SCI and 100 EI), and more than 80 key scientific research projects undertaken by aviation and aerospace research plants and institutes. In addition, he has undertaken a major project of two engines, a number of national major project plans and a sub-project of a major project of two engines. His research interests include aero-engine dynamic mathematical model, control system modeling, control law design, control system fault diagnosis, and fault tolerant design.

SHUBO YANG was born in Urumqi, China. He received the Ph.D. degree in engineering from Beihang University, in 2020. He is currently a Postdoctoral Researcher with Beihang University. His current research interests include control design, dynamic system modeling, and simulation.